

Vibration and motion control design and trade-off for high-performance mechatronic systems

Diederik Verscheure*, Bart Paijmans†, Hendrik Van Brussel*, Jan Swevers*

Abstract—This paper discusses the H_∞ -based design of a vibration controller for an industrial pick-and-place machine. A vibration controller is added to the classical motion control scheme with the purpose of improving positioning behavior by reducing the vibration level and settling time. It is shown that a trade-off is required between vibration reduction and motion control. The approach is validated experimentally and the results clearly illustrate the benefit of the proposed method.

I. INTRODUCTION

High-speed, high-accuracy operation and low-cost construction are the main thrusts behind the design of light-weight robotic manipulators, pick-and-place machines, etc. Light-weight structures operating at high speeds may suffer from significant vibration problems, thus degrading positioning accuracy and exhibiting large settling times. Furthermore, the dynamic behavior of a machine tool can depend on the position of the tool in its workspace. High-performance motion controllers that take into account these varying dynamics are needed.

This paper discusses the design of controllers to enable fast point-to-point movements for a pick-and-place machine with position-dependent dynamics. Various approaches address positioning of flexible structures have been proposed, ranging from optimal regulators [4][5] to input preshaping methods [7]. [15] improves positioning with H_∞ -based motion controllers, designed using a model matching approach. In this paper, the classical motion control scheme is extended with a vibration controller, to improve positioning performance, by

reducing the vibration level and settling time. This approach requires a trade-off between vibration and motion control. The design is explained for linear time-invariant (LTI) systems and the position-dependent dynamics can be taken into account using gain scheduling [10]. The implementation of a gain scheduling technique for the considered setup is addressed in [1].

The outline of this paper is as follows. Section II discusses the experimental setup and identification of linear models. The control structure and design approach are explained in section III. The design of a vibration and a motion controller is presented in section IV and section V respectively. Section VI discusses the experimental results and the trade-off between vibration reduction and motion control. Finally, conclusions and future work are presented.

II. EXPERIMENTAL SETUP

A. Description of the setup

The considered test-case is an industrial 3-axis pick-and-place machine shown in Fig. 1. The Y-motion is gantry driven by two linear motors (1). The X-motion of the carriage over the gantry is also driven by a linear motor (2). The vertical Z-motion is actuated by a rotary brushless DC-motor which drives a vertical beam by a ball screw/nut combination (3). The position of the linear motors and the length of the beam are measured with optical encoders and the acceleration in the X-direction of the end point of the beam (4), is measured with an accelerometer.

The objective is to position the end point of the beam as accurately and quickly as possible. However, fast movements of the linear motors excite the eigenfrequencies of the flexible beam and during motion, the length of the beam can continuously

* D. Verscheure, H. Van Brussel and J. Swevers, K.U.Leuven, Mechanical Engineering Department, division PMA diederik.verscheure@mech.kuleuven.be

† Bart Paijmans, Flanders Mechatronics Technology Center bart.paijmans@fmtc.be

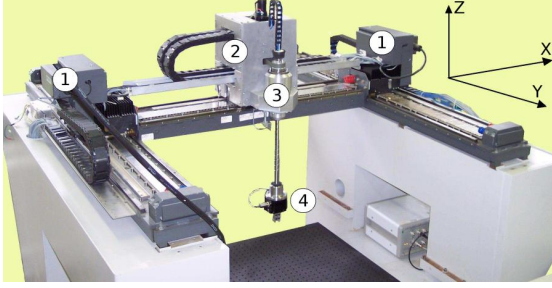


Fig. 1. Picture of the setup

change, giving rise to varying resonance frequencies. This paper focuses on motion and vibration control in the X-direction for fixed values of the length of the beam in the Z-direction.

B. Identification of linear models

The setup is identified for different beam lengths. For each length, two frequency response functions (FRFs) are measured using multi-sine excitation [11]. The X-motor has one input, the applied force, and two outputs, the motor position and the acceleration of the end point of the beam. The FRF motor position / motor force for different beam lengths is shown in Fig. 2. A mass-line characteristic (-40 dB/decade) is seen in the mid-frequency range. For lower frequencies, the slope tends to -20 dB/decade due to the presence of viscous and hysteretic friction [13]. For higher frequencies, the FRF exhibits a varying resonance, which is the first eigenfrequency of the beam. The FRF end point acceleration / motor force for different beam lengths, is shown in Fig. 3. Below the eigenfrequency of the beam, the acceleration of the end point is approximately the same as the motor acceleration. Above this eigenfrequency, the acceleration of the end point of the beam lags behind the acceleration of the motor. Linear models are estimated for the measured FRFs. A model of order 8 is used for the FRF motor position / motor force:

$$G_{POS} = \frac{K}{m \cdot s^2 + c \cdot s} \cdot \prod_{i=1}^3 \left(\frac{s^2}{\omega_{1,i}^2} + \frac{2 \cdot \zeta_{1,i} \cdot s}{\omega_{1,i}} + 1 \right). \quad (1)$$

The first part of the expression accounts for the low-frequency behavior of the motor and

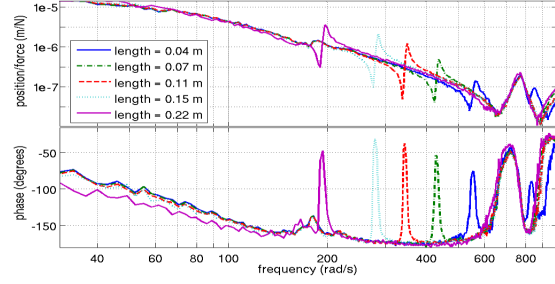


Fig. 2. The FRF motor position / motor force

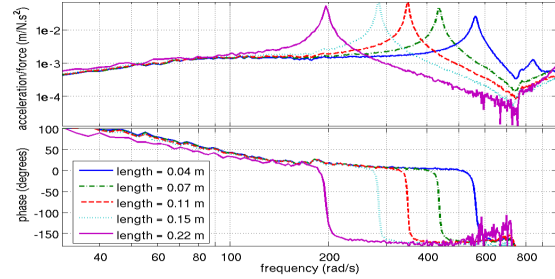


Fig. 3. The FRF end point acceleration / motor force

the other second order factors in the numerator and denominator account for the three antiresonance/resonance pairs seen in Fig. 2. The lowest antiresonance/resonance pair depends on the beam length and the two pairs at higher frequencies account for the effect of machine frame resonances. A model of order 4 is used for the FRF end point acceleration / motor force:

$$G_{ACC} = \frac{K \cdot s^2}{(m \cdot s^2 + c \cdot s) \cdot \left(\frac{s^2}{\omega_{2,1}^2} + \frac{2 \cdot \zeta_{2,1} \cdot s}{\omega_{2,1}} + 1 \right)}. \quad (2)$$

For low frequencies, this model coincides with the model relating motor force to motor acceleration and the additional term of order two in the denominator takes into account the eigenfrequency of the beam. For each FRF and each beam length, the parameters K , m , c , $\omega_{k,l}$ and $\zeta_{k,l}$ are estimated using a nonlinear least squares algorithm [11].

III. CONTROL STRUCTURE

The discussion in the following sections focuses on the design of controllers for one fixed beam length. The same procedure can be readily applied for other beam lengths. Subsection III-A discusses the control structure to improve positioning and subsection III-B explains the design approach.

A. Control structure

As shown by previous studies [8][12], an appropriate way of combining vibration and motion control is to use a HAC-LAC structure [9] as depicted in Fig. 4. A HAC-LAC structure consists of a high-authority motion controller C (HAC), built around the system with a low-authority vibration controller D (LAC). The purpose of the vibration controller is to assure that the acceleration of the end point of the beam ACC tracks a reference acceleration R_{ACC} , which is taken to be zero, but can also be used for acceleration feedforward. The motion controller C is a lead-lag controller [3], used to control the position of the motor POS and to track a reference position R_{POS} .

B. Design approach

If the influence of the eigenfrequency of the beam on the FRF motor position / motor force is quite negligible as in [12], a decoupled design of the motion and vibration controller is possible. In this paper, the influence of the varying resonance is not negligible, as seen in Fig. 2. Hence, the design of the HAC-LAC structure cannot be decoupled and is carried out as a two-stage procedure, based on the modeled transfer functions G_{ACC} and G_{POS} .

These models may differ from the actual FRFs \tilde{G}_{ACC} and \tilde{G}_{POS} , as indicated in Fig. 4, either due to model mismatches or slight variations of the beam length. Firstly, only the control scheme within the dash-dotted rectangle in Fig. 4 is considered and the vibration controller D is designed, while the motion controller C is omitted in this stage. The input of this closed-loop system is the reference acceleration R_{ACC} for the end point of the beam. The outputs are the motor position and the acceleration of the end point.

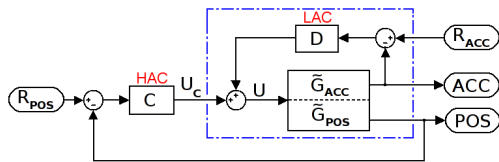


Fig. 4. The control scheme

Secondly, the motion controller C is designed around the system contained within the dash-dotted

rectangle in Fig. 4, namely the original system, augmented with the vibration controller D . The design of the vibration and the motion controller is discussed in section IV and section V respectively.

IV. DESIGN OF THE VIBRATION CONTROLLER

A. Design considerations

The vibration controller needs to be active only in a frequency range around the eigenfrequency of the beam. The control action should be small below the eigenfrequency, to minimize interference with the motion controller and to limit the influence of the accelerometer measurements, which are generally less accurate at low frequencies. Additionally, to limit noise sensitivity and prevent actuator saturation, the control action of the vibration controller should be small at frequencies well above the eigenfrequency. Around the eigenfrequency of the beam, the end point acceleration ACC needs to track the reference acceleration R_{ACC} as closely as possible and good disturbance rejection is desired, implying that the sensitivity $S = \frac{1}{1+D \cdot G_{ACC}}$ should be as small as possible [6]. This in turn implies that the complementary sensitivity $T = \frac{D \cdot G_{ACC}}{1+D \cdot G_{ACC}}$ is around unity (0 dB) in this frequency range, since $S + T = 1$. However, this range cannot be made arbitrarily narrow, as this leads to peaking of the sensitivity S [6], which is undesirable. as expressed by Doyle's stability robustness criterion [2]:

$$\left| \frac{G_{ACC}(j\omega) - \tilde{G}_{ACC}(j\omega)}{\tilde{G}_{ACC}(j\omega)} \right| < \left| \frac{1}{S(j\omega)} \right|. \quad (3)$$

Here, S is the sensitivity calculated from the modeled transfer function G_{ACC} and a given controller D and \tilde{G}_{ACC} is the actual transfer function. This inequality expresses that stability for the closed-loop system is only guaranteed for relative mismatches of G_{ACC} that are smaller than $\left| \frac{1}{S(j\omega)} \right|$.

A certain degree of robustness is required, especially if the controller is used in conjunction with gain scheduling. In linearization gain scheduling [10], controllers are designed for an LTI system at a fixed operating point of the scheduling variable, in this case the length of the beam, but are used in a range around this design point. For this reason,

performance robustness is equally desirable. For a given vibration controller D , the following equality holds [6]:

$$\frac{T(j\omega) - \tilde{T}(j\omega)}{\tilde{T}(j\omega)} = S(j\omega) \cdot \frac{G_{ACC}(j\omega) - \tilde{G}_{ACC}(j\omega)}{\tilde{G}_{ACC}(j\omega)}, \quad (4)$$

where \tilde{T} is the complementary sensitivity calculated from the actual transfer function \tilde{G}_{ACC} . This equation expresses that the complementary sensitivity, representing the closed-loop performance, will vary little as a consequence of relative mismatches of G_{ACC} , wherever S is small. As a result, stability robustness and performance robustness are obtained by making S small. However, to limit interference with the motion controller, the frequency range in which this is realized, cannot be too wide.

B. H_∞ -design of the vibration controller

A vibration controller D is determined for a beam length of 0.15m, using an H_∞ -based approach by solving the mixed sensitivity problem [6][14]. In the SISO case, this problem can be solved by finding the controller D that minimizes [6]:

$$\sup_{\omega \in \mathbb{R}} (|W_1(j\omega)S(j\omega)|^2 + |W_2(j\omega)T(j\omega)|^2), \quad (5)$$

with W_1 and W_2 suitably chosen, stable, rational functions of $j\omega$. If γ^2 is defined as the minimum value of (5), then the optimal solution satisfies:

$$|S(j\omega)| \leq \frac{\gamma}{|W_1(j\omega)|}, \quad \omega \in \mathbb{R}, \quad (6)$$

$$|T(j\omega)| \leq \frac{\gamma}{|W_2(j\omega)|}, \quad \omega \in \mathbb{R}. \quad (7)$$

Define τ_0 as the inverse of the eigenfrequency of the beam. The right-hand side of (7) presents an upper bound for T . To minimize interference with the motion controller, T needs to be smaller than unity outside the frequency range of the eigenfrequency of the beam. To this end, $1/W_2$ can be chosen as a symmetric weighting function of order $2n$ with a maximum amplitude at $1/\tau_0$:

$$\frac{1}{W_2} = \frac{\alpha \cdot \prod_{i=1}^n (\tau_0 \cdot \lambda_i \cdot s + 1) \cdot (\tau_0 / \lambda_i \cdot s + 1)}{\prod_{j=1}^n (\tau_0 \cdot \mu_j \cdot s + 1) \cdot (\tau_0 / \mu_j \cdot s + 1)}. \quad (8)$$

α is chosen such that $1/W_2$ attains a value around 0 dB at $1/\tau_0$ and $\lambda_i > \mu_j > 1$. n and μ_j determine

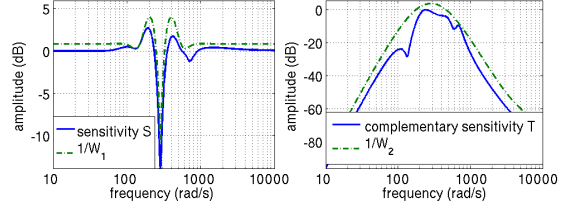


Fig. 5. The upper bounds $1/W_1$ (left) and $1/W_2$ (right), for the sensitivity S and the complementary sensitivity T

the width of the peak and λ_i are chosen sufficiently larger than μ_j . The weighting function $1/W_2$ is shown in Fig. 5 on the right, where $n = 4$, $\alpha = 1.5$, $\lambda_i \approx 17$ and $\mu_j \approx 1.05$. Inequality (7) is usually dominant outside the frequency band around the eigenfrequency of the beam. Hence, the high- and low-frequency shape of $1/W_2$ is most important.

To obtain a small S around the eigenfrequency of the beam, a lower bound T_l on the complementary sensitivity is chosen firstly. As $1/W_2$ is an upper bound for T for all $0 < \gamma \leq 1$, T_l can be determined from (8) by decreasing α , decreasing μ_j , increasing the order n or by a combination of the above, allowing for many degrees of freedom to shape T_l . From T_l , $1/W_1$ may be calculated as follows:

$$\frac{1}{W_1} = \eta \cdot (1 - T_l), \quad (9)$$

where $\eta \geq 1$ is introduced to ensure that the upper bound for S in (6) is not too restrictive. The weighting function $1/W_1$ is shown in Fig. 5, where $1/W_1$ is calculated from (9) with $\eta = 1.1$ and T_l is calculated from (8) with $n = 8$ and $\alpha = 0.7$. Inequality (6) is usually dominant in the frequency range around the eigenfrequency, hence the shape of $1/W_1$, is important in this range.

Based on these weighting functions, an H_∞ -controller is determined using the MATLAB Robust Control Toolbox. In Fig. 5, the resulting sensitivity S and complementary sensitivity T are compared with the inverse of the chosen weighting functions. It can be seen that (7) and (6) are satisfied for $\gamma = 1$.

V. DESIGN OF THE MOTION CONTROLLER

A. Identification with the vibration controller

The FRFs of the system with the vibration controller can be calculated from the transfer functions

G_{POS} , G_{ACC} and D or can be measured by applying an excitation signal to the system within the dash-dotted rectangle in Fig. 4. The input signal U to the motor is the sum of the excitation signal U_C and the control signal of the vibration controller. The reference acceleration R_{ACC} is kept equal to zero. The FRFs motor position / U_C and end point acceleration / U_C are shown in full line in Fig. 6 to the left and right respectively. Both FRFs are compared to those without the vibration controller, in dash-dotted lines. For the FRF end point acceleration / U_C , the vibration controller realizes increased damping of the eigenfrequency and for the FRF motor position / U_C , almost complete suppression of the resonance frequency is obtained.

B. Design of the motion controller

A lead-lag controller [3] is first designed for the system without vibration controller, resulting in a bandwidth of 25 Hz and phase margin of 46° for the motion control loop. The resulting loop transfer function is shown in Fig. 7 on the left. The addition of the vibration controller causes an extra phase lag near the eigenfrequency of the beam in the FRF motor position / U_C , shown in full line in Fig. 6 and has important consequences for the bandwidth of the motion controller. To obtain a bandwidth above or near the eigenfrequency of the beam, it is necessary to add a second lead term to the lead-lag controller, to compensate for this phase lag. This results in a reduction of the vibration suppression, as the second lead term mainly compensates for the effect of the vibration controller. Additionally, it also causes the peaks of the high-frequency machine frame resonances to rise above 0 dB, deteriorating the phase margin and resulting in unacceptable excitation of these resonances. Therefore, there is little choice but to select a bandwidth that is lower than the eigenfrequency of the beam. A standard lead-lag controller is sufficient in this case and is designed to yield a bandwidth of 10 Hz and a phase margin of 55° . The loop transfer function with the vibration controller is shown in Fig. 7 on the right.

VI. EXPERIMENTAL VALIDATION

The performance of the vibration controller is validated experimentally for two cases. In the first

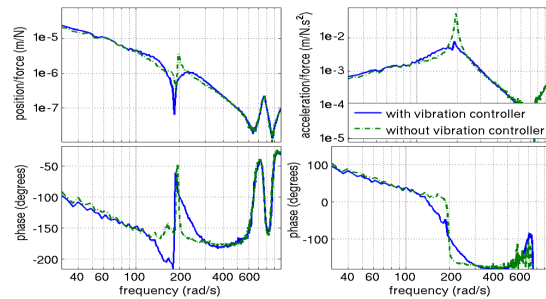


Fig. 6. The FRF motor position / excitation force U_C (left) and end point acceleration / excitation force U_C (right)

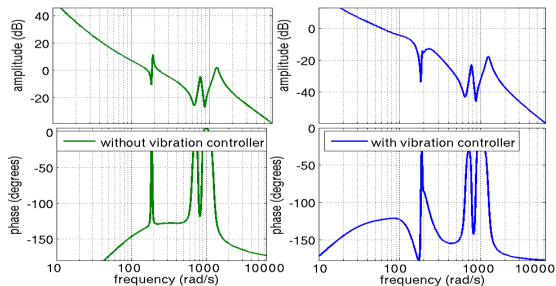


Fig. 7. The loop transfer function of the motion control loop with (left) and without (right) vibration controller

case, a high-bandwidth lead-lag controller, designed for the system without vibration controller, is used. To evaluate the performance, a step in the reference position R_{POS} is applied to the motion control loop and the acceleration of the end point of the beam is measured both with and without the vibration controller. The acceleration response of the end point is shown in Fig. 8. In the second case, a low-bandwidth lead-lag controller, designed for the system with the vibration controller, is used and the above experiment is repeated. The result is shown in Fig. 9. A high-bandwidth motion controller excites the eigenfrequency of the beam more, since the maximum amplitude of the acceleration is higher. Adding a vibration controller does not significantly improve the settling time, due to interference between vibration and motion controller.

In the case of a low-bandwidth motion controller, the presence of a vibration controller considerably improves the settling time. This improvement shows that it is particularly useful to incorporate a vibration controller in the control scheme, for applications that require many short point-to-point

movements. Although using a vibration controller requires lowering of the bandwidth of the motion controller, nevertheless, faster positioning can be achieved by a reduced settling time of the end point of the beam.

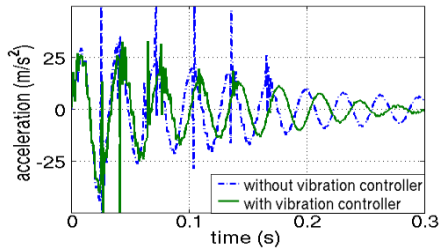


Fig. 8. Acceleration of the end point with and without the vibration controller, for a high-bandwidth motion controller.

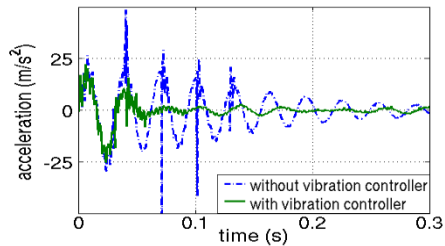


Fig. 9. Acceleration of the end point with and without the vibration controller, for a low-bandwidth motion controller.

VII. CONCLUSIONS AND FUTURE WORK

A pick-and-place machine with structural flexibilities is identified and controlled so as to achieve fast and accurate positioning. Improved positioning behavior is obtained by incorporating a vibration controller into the motion control scheme. The controller design consists of two stages. Firstly, a vibration controller is designed whereby considerations concerning robustness and stability and limiting interference with the motion controller are taken into account. Secondly, a motion controller is tuned for the system augmented with the vibration controller, whereby a more conservative choice of bandwidth of the motion controller is required, due to the phase lag introduced by the vibration controller. Nevertheless, the experimental results indicate the benefit of this approach and the successive design stages illustrate the ease of the overall

method. Ongoing and future research focuses on the combination of different LTI controllers using gain scheduling [1], in order to achieve fast and accurate positioning for a variable length of the beam.

VIII. ACKNOWLEDGEMENTS

This research is sponsored by the Belgian programme on Interuniversity Poles of Attraction (IAP5/06: AMS).

REFERENCES

- [1] B. Paijmans, W. Symens, H. Van Brussel, J. Swevers, A gain-scheduling-control technique for mechatronic systems with position-dependent dynamics, *Proc. Am. Contr. Conf.*, Vol. 25, 2006 (accepted and to appear)
- [2] J.C. Doyle, *Robustness of Multiloop Linear Feedback Systems*, *Proc. IEEE Conf. Dec. Contr.*, San Diego, CA, 1979.
- [3] G. Franklin, J.D. Powell and A. Emami-Naeini, *Feedback control of dynamic systems*, Prentice Hall, 4th ed., 2002.
- [4] S. Hara, K. Yoshida, Simultaneous Optimization of Positioning and Vibration Control using a Time-varying Frequency-Shaped Criterion Function, *Control Eng. Practice*, Vol. 4, No. 4, pp. 553-561, 1996.
- [5] S. Hara, K. Nakamura, T. Narikiyo, Positioning and Vibration Control of Time-Varying Vibration Systems by Means of Nonstationary Optimal Regulator, *Proc. of DETC'03*, Chicago, Illinois, 2003.
- [6] O.H. Bosgra and H. Kwakernaak, *Design Methods for Control Systems*, Lecture Notes for a course, Dutch Institute of Systems and Control, The Netherlands, 2005.
- [7] B. K. Kim, S. Park, W. K. Chung, Y. Youm, Input Preshaping Vibration Suppression of Beam-Mass-Cart Systems Using Robust Internal-Loop Compensator, *Proc. Int. Conf. Rob. Autom.*, Seoul, Korea, 2001.
- [8] B. Present, W. Verlinden, Motion and vibration control of a flexible structure, Master's Thesis, Dept. Mech. Eng., K.U.Leuven, Belgium, 1999.
- [9] A. Preumont, *Vibration Control of Active Structures*, Kluwer Academic Publishers, Dordrecht, 1997.
- [10] W.J. Rugh and J.S. Shamma, Research on gain scheduling, *Automatica*, Vol. 36, pp.1401-1425, 2000.
- [11] J. Schoukens and R. Pintelon, *System identification: a frequency domain approach*, IEEE Press, Piscataway, 2001.
- [12] W. Symens, H. Van Brussel, J. Swevers, B. Paijmans, Gain-scheduling control of machine tools with varying structural flexibilities, *Proc. ISMA*, Leuven, Belgium, 2004.
- [13] W. Symens, Motion and vibration control of mechatronic systems with variable configuration and local non-linear friction, Ph.D. Thesis, Dept. Mech. Eng., K.U.Leuven, Belgium, 2004.
- [14] M. Verma and E. A. Jonckheere, L_∞ -Compensation with Mixed Sensitivity as a Broadband Matching Problem, *Systems and Control Letters*, Vol. 4, pp. 125-129, 1984.
- [15] X. Yang, D. G. Taylor, H_∞ Control Design for Positioning Performance of Gantry Robots, *Proc. Am. Contr. Conf.*, Vol. 5, Chicago, Illinois, 2000.